

Permanent Magnet Synchronous Motor Design Using Grey Wolf Optimizer Algorithm

Yannis L. Karnavas, Ioannis D. Chasiotis, Emmanouil L. Peponakis

Laboratory of Electrical Machines, Department of Electrical and Computer Engineering,
Democritus University of Thrace, Xanthi, Hellas (GR)

Article Info

Article history:

Received Dec 22, 2015

Revised Mar 21, 2016

Accepted Apr 16, 2016

Keyword:

PM synchronous motor
Electrical machines design
High efficiency motors
Meta-heuristic optimization
FEM analysis

ABSTRACT

Common high-torque low-speed motor drive schemes combine an induction motor coupled to the load by a mechanical subsystem which consists of gears, belt/pulleys or camshafts. Consequently, these setups present an inherent drawback regarding to maintenance needs, high costs and overall system deficiency. Thus, the replacement of such a conventional drive with a properly designed low speed permanent magnet synchronous motor (PMSM) directly coupled to the load, provides an attractive alternative. In this context, the paper deals with the design evaluation of a 5kW/50rpm radial flux PMSM with surface-mounted permanent magnets and inner rotor topology. Since the main goal is the minimization of the machine's total losses and therefore the maximization of its efficiency, the design is conducted by solving an optimization problem. For this purpose, the application of a new meta-heuristic optimization method called "Grey Wolf Optimizer" is studied. The effectiveness of the method in finding appropriate PMSM designs is then evaluated. The obtained results of the applied method reveal satisfactorily enhanced design solutions and performance when compared with those of other optimization techniques.

Copyright © 2016 Institute of Advanced Engineering and Science.
All rights reserved.

Corresponding Author:

Yannis L. Karnavas,
Lab. of Electrical Machines, Department of Electrical and Computer Engineering,
Democritus University of Thrace,
Office 0.21, Build. B, Campus, Kimmeria, GR-671 00, Xanthi, Hellas (GR).
Email: karnavas@ee.duth.gr

1. INTRODUCTION

Three phase induction motors used to be (and mainly still are) the most popular motors used in consumer and industrial applications. Their installed capacity is impressive; it accounts for approximately 70% of the worldwide industrial energy consumption [1]. Nowadays however, the environmental concern increases continuously and at the same time global economy plays an important role as it is getting more and more strict. Thus, electrical drives with higher efficiency and lower costs are strongly desirable [2],[3]. In this context, the replacement of induction machines with permanent magnet synchronous motors (PMSM) seems to be a very attractive alternative. This alternative can be justified by several reasons: a) PMSM are capable of producing very high starting torque, b) current drawn by PMSM is directly proportional to torque so they can be controlled directly from current reading (this is not possible with induction motor), c) they provide higher flux density than comparable induction motors, d) they exhibit a wider speed range than induction motors, e) the gearbox can be eliminated in low speeds i.e. lower than 500rpm, f) PMSM don't have rotor winding resulting in at least 20% lower copper losses and consequently higher efficiency, g) considerable savings in power consumption and lower noise pollution and h) relatively low price of the magnetic materials used [4],[5]. This study focuses on low-speed drives without a gearbox, which are also called "direct drives". Typical applications of low-speed direct drives to which permanent magnet machines may be used, include wind turbines, elevators, trams, boat propulsion, and waste water treatment plants. Direct drives for wind

turbine generators have been studied i.e. in [6]-[8]. A boat propulsion system consisting of an 100kW PMSM is designed and analyzed in [9]. An axial flux PMSM for an elevator system is proposed in [10] and an application of PMSM in traction-tram application can be found in [11]. Also, a PMSM for waste water direct-drive mixer motor is thoroughly discussed in [12],[13]. From the above, it is apparent the the PMSM design problem has received great attention the last years.

On the other hand, the application of meta-heuristic optimization techniques have become very popular over the last two decades, especially those based on swarm intelligence i.e. genetic algorithms (GA), particle swarm optimization (PSO) and ant colony optimization (ACO). Variants of them have been applied in many fields including the solving of electrical machines design problems [14]-[16]. There are four main reasons that meta-heuristic have become remarkably wide-spread [17],[18]. Firstly they are quite simple because they have been inspired by simple concepts with respect to physical phenomena, animals' behaviors, or evolutionary concepts. Secondly they are flexible. Their flexibility refers to their applicability to different problems without any special changes in the structure of the algorithm. Thirdly, most of them provide derivation-free mechanisms and thus optimize problems stochastically, in contrast to gradient-based optimization approaches. Finally, they present local optima avoidance capability compared to conventional optimization techniques. This is due to their stochastic natures which allow them to avoid stagnation in local solutions and search the entire search space extensively.

One of the most recent meta-heuristic has been proposed by Mirjalili *et al* and is called "Grey Wolf Optimizer" (GWO) [19]. This paper aims to investigate and present the effectiveness of GWO algorithm in the complex problem of finding a high-efficient suitable radial flux surface PMSM design to be used as a replacement of a traditional induction motor-gearbox low speed drive system. The motivation lies mainly in a) the fact that, to the authors knowledge extend, similar works haven't found yet in literature and b) the concept that a particular meta-heuristic may show very high promising results on certain problems but at the same time may show poor performance on different set of problems [20],[21]. The paper is organized as follows: The problem formulation (geometrical, magnetic and electrical properties) of the PMSM design procedure is presented first at Section 2. Once the optimization problem has been set, the brief preliminaries of the adopted method are shown in Section 3. Continuing, the design variables are decided, the constants and the relevant constraints are defined, the proposed cost function is presented and the corresponding results are shown and compared next in Section 4. The results are commented and finally the work is concluded in Section 5.

2. PMSM MODEL AND PROBLEM FORMULATION

Radial flux's PMSM are quite conventional PM machines and they are widely used for direct-driven applications. In these machines, the flux flows radially inside the machines while the current flows in the axial direction. The permanent magnets are placed on the rotor surface (outer circumference of the rotor). Figure 1a shows a general cross section of the configuration under study here. The geometrical representation refers to the outer diameter of the machine (D_o), the inner stator diameter (D_s), the rotor diameter (D_r), the magnet length (l_m), the pole angle (2θ), and the airgap length (δ). Figure 1b depicts a more detailed geometry of the PMSM with inner rotor regarding slots. Here, it is seen the slot pitch (τ_s), the stator slot height (h_{ss}), the stator yoke height (h_{sy}), the stator teeth height (h_{sw}), the stator slot opening (b_{ss0}), the stator slot width at start (b_{ss1}), the stator slot width at end (b_{ss2}) and the stator teeth width (b_{st}).

We denote as Q_s the number of stator slots. Then the slot pitch τ_s can be defined as $\tau_s = D_s/Q_s$. From this point on, the following calculations can be applied.

$$D_s = D_r + 2l_m + 2\delta \quad , \quad h_{sy} = \frac{1}{2}(D_o - D_s - 2h_{ss}) \quad , \quad A_s = \frac{1}{2}(b_{ss1} + b_{ss2})(h_{ss} - h_{sw}) \quad (1)$$

$$b_{ss1} = f \frac{D_s + 2h_{sw}}{Q_s} - b_{st} \quad , \quad b_{ss2} = f \frac{D_s + 2h_{ss}}{Q_s} - b_{st} \quad (2)$$

where A_s is the slot area. Also, since the inner stator diameter D_s is very large compared to the slot pitch τ_s , the relevant slot widths (which are actually arcs of circles) are approximated as straight lines in Eqs. (2). It can be seen that the 2-dimensional geometrical structure of the stator can be described entirely if the following parameters: D_o , D_r , b_{st} , b_{ss0}/b_{ss1} ratio, h_{sw} , h_{ss} , l_m , θ , and Q_s are obtained. By adding the number of poles p , the half pole angle θ and the active length L , the whole 3-dimensional geometry can be described.

2.1. Magnetic properties

The PMSM design procedure relies on the amplitude of the fundamental airgap flux density and thus its

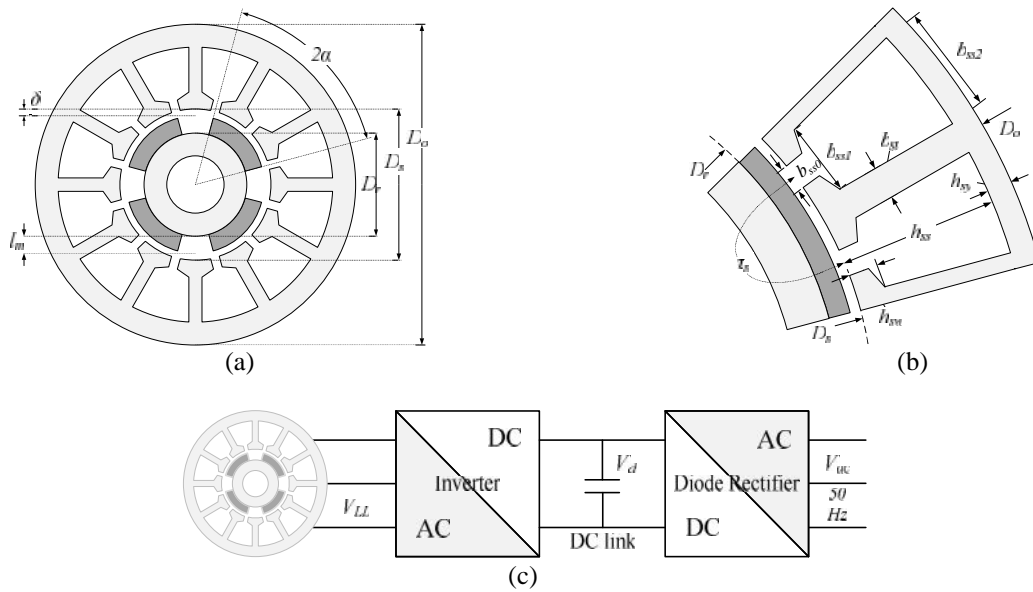


Figure 1. Representation of the design problem considered: a) inner rotor PMSM cross section, b) detailed geometry of slots, airgap and permanent magnets (one pole) and (c) typical PMSM drive system.

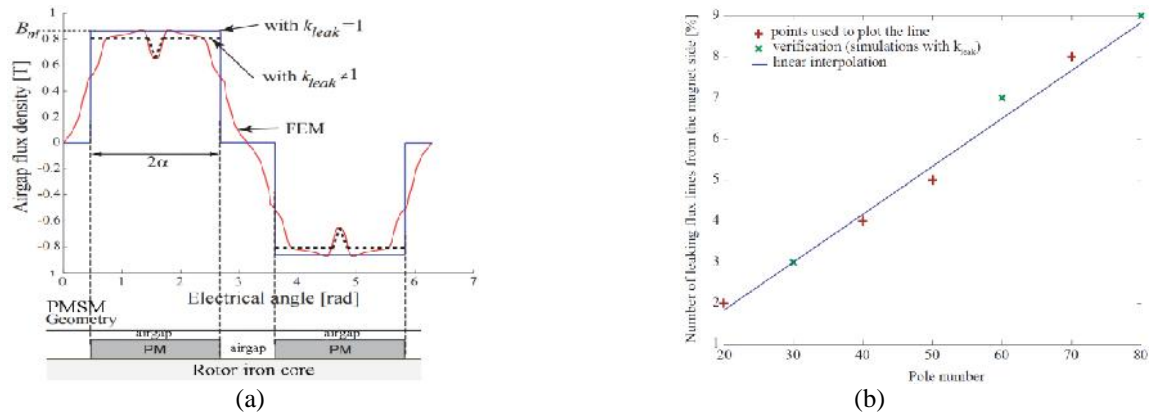


Figure 2. Magnetic considerations of PMSM design: a) airgap flux density variation with and without considering magnetic leakage, b) approximation of magnetic leakage as a function of poles number

Calculation should be conducted. For surface mounted permanent magnet motor designs the airgap flux density is assumed to have a rectangular shape (as wide as the magnet width) and a maximum value of B_m as depicted in Figure 2a. This value can be calculated as:

$$B_m = B_r k_{leak} \left(\mu_r k_C^{-1} \left(l_m \left(\frac{l_s - b_{ss0}^2}{b_{ss0} + 5u} \right) \right)^{-1} + 1 \right)^{-1} \tag{3}$$

where B_r is the remanence flux density of the magnet, k_{leak} is the leakage factor (the percentage of the flux lines which pass through the airgap), μ_r is the relative magnet permeability and k_C is the Carter factor. The Carter factor can be derived from [22] and is shown in Eq. (4), along with the leakage factor which can be obtained through magneto-static FEM simulations. A linear approximation of k_{leak} dependency on the poles

number p has been found in [13] as illustrated in Figure 2b and it is also used here:

$$k_c = \left(\frac{b_{ss0}^2}{b_{ss0} + 5u} \right)^{-1}, \quad k_{leak} = 1 - (7p/59.5)/100 \quad (4)$$

2.2. Electrical and thermal properties

The design problem formulation is finalized by defining the electrical parameters of the PMSM i.e. inductances, stator's resistance, supply and induced voltages, ampere-turns and current density. This kind of motors is of a non salient type and thus the d -axis and q -axis synchronous inductances are equal. Moreover, $L_d=L_q=L_l+L_{md}=L_l+L_{mq}$, and the leakage inductance (L_l) and the magnetizing reactances (L_{md} , L_{mq}) are [22]:

$$L_l = pqn_s^2 L_{l0} \lambda_1, \quad L_{md} = \frac{3}{f} (qn_s k_{w1})^2 \sim_0 \left(u k_c + \frac{L_m}{\tau_r} \right)^{-1} (D_s - u) L \quad (5)$$

where q is the number of slots per pole per phase, n_c is conductors per slot number, λ_1 is the specific permeance coefficient of the slot opening depending on the slot geometry, k_{w1} is the fundamental winding factor (equal to unity for $q=1$) and L is the active machine length. Furthermore, the induced voltage rms value along with the corresponding stator winding per phase resistance can be evaluated by

$$E = (1/\sqrt{2}) \tilde{S} k_{w1} q n_s B_m L (D_s - u), \quad R = \dots_{cu} n_s^2 q (pL + k_{ew} f (D_s + h_{ss})) (f_s A_s)^{-1} \quad (6)$$

where f_s is the slot fill factor equals to 0.45 for distributed windings and k_{ew} is the end-winding factor [23]. Finally, the ampere-turns are derived from the peak current loading,

$$n_s I = 4T_s \left(f (D_s - u)^2 L B_u k_{w1} k_{sl} \right)^{-1} \quad (7)$$

where k_{sl} is a slot leakage loss compensating factor which equals to 0.95 for inner rotor configuration. Now, the current density and the supply voltage across one phase can be derived using the corresponding vector diagram ($I_q=I$), and are therefore given by,

$$J = n_s I (A_s f_s)^{-1}, \quad V = \sqrt{\left(|E| + R |I_q| \right)^2 + \left(L_q \tilde{S} |I_q| \right)^2} \quad (8)$$

Each value should not exceed the maximum allowable slot current density (J_{max}). It is known that, for air-cooled machines, this value is about 800A/cm², while for forced cooling J_{max} is allowed to be more than 1kA/cm². It should be noted also that voltage V in Eq. (8), is actually the inverter's output voltage according to Figure 1c. Even for a "bad" scenario of 50% modulation ratio, the V_{LL} is about 30% of the rectified dc voltage across the capacitor. Thus, V is approximately taken as 86.55Volts.

3. OPTIMIZATION AND APPLIED METHODS

The problem stated above is actually a constrained optimization problem. In a mathematical notation and without loss of generality can be described as [24],

$$\text{minimize } f(\mathbf{x}), \quad \mathbf{x} = (x_1, x_2, \dots, x_n) \in \mathbf{R}^n \quad (9)$$

where $\mathbf{x} \in W \subseteq S$. The objective function f is defined on the search space $S \subseteq \mathbf{R}^n$. The sets $W \subseteq S$ and $Y = S - W$, define the feasible and infeasible search spaces respectively. Usually, the search space S is defined as an n -dimensional rectangle in \mathbf{R}^n (domains of variables defined by their lower and upper bounds):

$$x_j^{lb} \leq x_j \leq x_j^{ub}, \quad j = 1, 2, \dots, n \quad (10)$$

Whereas the feasible set $W \subseteq S$ is defined by a set of additional $P - 0$ constraints:

$$W = \left\{ \mathbf{x} \mid \begin{cases} g_k(\mathbf{x}) \leq 0 ; h_j(\mathbf{x}) = 0 ; \\ k = 1, 2, \dots, L ; j = L + 1, \dots, P \end{cases} \right\} \quad (11)$$

Any point $\mathbf{x} \in W$ is called a feasible solution; otherwise, \mathbf{x} is an infeasible solution.

3.1. Gray wolf optimization (GWO)

As it is claimed by the authors in [19], the main advantage of GWO algorithm over most of the well-known meta-heuristic algorithms is that the GWO algorithm operation requires no specific input parameters and, additionally, it is straightforward and free from computational complexity. Further, its advantages include ease of transformation of such concept to the programming language and ease of comprehensibility. But, as it was stated in the Introduction, there is no meta-heuristic optimization technique well suited for all optimization problems. For this reason, we examine here the GWO suitability for the optimization problem described previously. The GWO algorithm mimics the leadership hierarchy and hunting mechanism of gray wolfes pack in nature. Four types of grey wolves such as *alpha* (α), *beta* (β), *delta* (δ), and *omega* (ω) are employed for simulating the pack leadership hierarchy. *Alpha* wolves represent the top-level i.e. the absolute leaders (which also give the best solution to the optimization problem). *Beta* wolves represent a second-level group in hierarchy which actually help *alphas* in decision making while at the same time command the other lower-level wolves. *Omega* wolfs refer to the lowest hierarchy level, thus the wolves belong to this group have to submit to all the other dominant wolves. Finally, if a wolf can not be characterized as α , β , or δ , he/she is called *delta*. *Delta* wolves have to submit to *alphas* and *betas*, but they dominate the *omega* ones. In a nature-context environment, the *delta* wolves may be scouts, elders, sentinels or caretakers. In addition to this social hierarchy, group hunting is the other basic characteristic of GWO, because it provides interesting social behaviour of grey wolves.

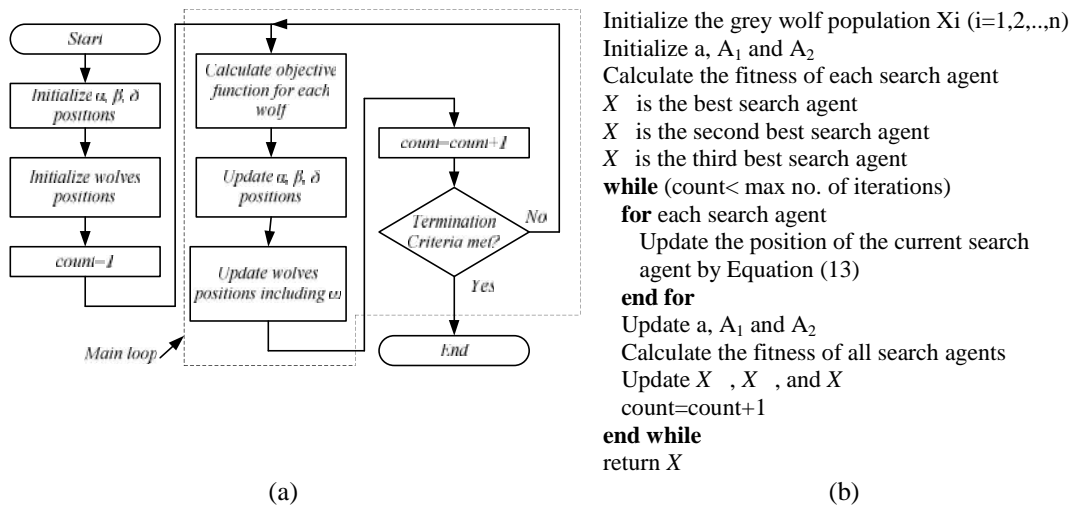


Figure 3. Simplified illustration of Grey Wolf Optimizer algorithm, a) flowchart, b) pseudo-code

There are three main steps of hunting, *searching for prey*, *encircling prey*, and *attacking prey*. The mathematical implementation of these steps to GWO (or modifications of them) is actual the mean of performing optimization in a complex problem. An illustration of the GWO algorithm in flowchart and pseudo-code form is depicted in Figure 3. The basic mathematical expressions used by GWO (prey's encircling behavior) is formulated by,

$$\begin{aligned} \mathbf{U} &= \left| \mathbf{A}_1 \mathbf{X}_{prey}(t) - \mathbf{X}_{wolf}(t) \right| & \mathbf{A}_1 &= 2\mathbf{r}_1 \\ \mathbf{X}_{wolf}(t+1) &= \mathbf{X}_{prey}(t) - \mathbf{A}_2 \mathbf{U} & \mathbf{A}_2 &= 2\mathbf{a}\mathbf{r}_2 \mathbf{a} \end{aligned} \quad (12)$$

where, \mathbf{X}_{prey} is the prey's position vector, \mathbf{X}_{wolf} is the grey wolves position vector, \mathbf{A}_1 , \mathbf{A}_2 are coefficient vectors, \mathbf{r}_1 , \mathbf{r}_2 are arbitrary vectors in gap $[0,1]$, \mathbf{a} is a vector linearly reduced from 2 to 0 during iterations and

t is any current iteration. Especially for vector \mathbf{A}_2 , it can take values in the gap $[-2\mathbf{a}, 2\mathbf{a}]$, so as when $|\mathbf{A}_2| < 1$ the wolves are forced to attack the prey. This is translated as the method's exploitation ability while searching for prey is the exploration ability. When $|\mathbf{A}_2| > 1$ the wolves pack is enforced to diverge from the prey. In any iteration, the wolves' position update is performed by,

$$\mathbf{X}_{wolf}(t+1) = (1/3) \begin{pmatrix} \mathbf{X}_{a_wolf}(t) - \mathbf{A}_{2(r_wolf)} \left| \mathbf{A}_{1(r_wolf)} \mathbf{X}_{r_wolf}(t) - \mathbf{X}_{wolf}(t) \right| + \\ \mathbf{X}_{s_wolf}(t) - \mathbf{A}_{2(s_wolf)} \left| \mathbf{A}_{1(s_wolf)} \mathbf{X}_{s_wolf}(t) - \mathbf{X}_{wolf}(t) \right| + \\ \mathbf{X}_{u_wolf}(t) - \mathbf{A}_{2(u_wolf)} \left| \mathbf{A}_{1(u_wolf)} \mathbf{X}_{u_wolf}(t) - \mathbf{X}_{wolf}(t) \right| \end{pmatrix} \quad (13)$$

3.2. Genetic Algorithms and Particle Swarm Optimization

For fair comparison purposes, two other meta-heuristic optimization techniques are also applied to the same problem, genetic algorithm (GA) and particle swarm optimization (PSO). These techniques have been proved robust and efficient enough to most engineering problems in the past. Moreover, since they are well-known, their principles of operation have been extensively presented in the literature and therefore no relative information is given here. The reader can refer to [25],[26] for further implementation details.

3.3. Objective functions and case studies

The desired PMSM characteristics are shown in Table A1 in the Appendix. Due to the large number of variable names, symbols etc., all the relevant information as well as the results obtained here will be presented in a tabularized form. From Figure 1 and Eqs. (1)-(8), it is derived that there are twelve design variables that are needed to be optimized by the applied algorithms. All the other quantities can be calculated implicitly. Table A2 in the Appendix shows these design variables, all of them related to the motor's geometry. In the same Table the upper and lower bounds of the variables are given. Additionally, Table A3 summarizes the constant values used in the calculations, while Table A4 presents the required problem constraints. A simple formulation for the objectives/cost functions (CF) to be minimized is proposed here as,

$$CF_n = S_k \cdot Q_k \rightarrow \begin{cases} CF_1 = [0.70 \quad 0.15 \quad 0.15] \cdot [M_w^{tot} \quad P_L^{tot} \quad M_m^{tot}]^T \\ CF_2 = [0.15 \quad 0.70 \quad 0.15] \cdot [M_w^{tot} \quad P_L^{tot} \quad M_m^{tot}]^T \\ CF_3 = [0.15 \quad 0.15 \quad 0.70] \cdot [M_w^{tot} \quad P_L^{tot} \quad M_m^{tot}]^T \end{cases} \quad (14)$$

where S_k is a $1 \times k$ row matrix containing the cost function's weight coefficients and Q_k is a $k \times 1$ column matrix containing any quantities under concern. It can be seen that this type of formulation can be expanded to more variables easily. Here, the quantities chosen are three ($k=3$): the total machine weight (M_w^{tot}), the total magnets weight (M_m^{tot}) and the total copper losses (P_L^{tot}). Furthermore, although numerous cost functions can be produced that way, three variations ($n=3$) are examined.

4. APPLICATION RESULTS AND DISCUSSION

Nine sets of optimization results were derived (3 methods x 3 objective functions) for the inner rotor PMSM design problem. Table 1 shows the twelve design variables through GWO, GA and PSO respectively and for each one of the cost functions applied (CF_1 - CF_3). From this Table it is initially clear that all algorithms succeeded in converging to a -near- optimum design solution satisfying all of the existing constraints. Also, compared to [21], these results, as well as those follow, are much better. For example, the outer diameter of the motor (D_o) is kept within satisfactory limits of 24-38cm, with a 20-50cm constraint, the machine length (L) found between 10-17cm only (with a 10-50cm constraint), while the magnet height (l_m) varied from 7.8mm to 12.8mm (with a 2-15mm constraint).

More compact information can be found in Table 2 which shows the motors total weight, their efficiency and the total magnets weight in each case, through the algorithms applied and for every cost function. It is seen that the corresponding quantities ranges (min-max) found to be 48.5kg-96.1kg, 74.8%-96.4% and 1.9kg-4.5kg respectively, by far less than the relative constraint. This Table reveals also the following:

- If the machine weight is the primary objective (cost function CF_1), the GWO solutions present the lighter (~48kg) and more efficient (~90%) motor, by keeping the magnet weight low enough (~2.7kg). The second "winner" in this case is GA, while for the PSO method present a little worse results than the GA.

- b) The same conclusions are valid in the case where the magnets weight is the primary objective (cost function CF_3). GWO method presents a solution with low magnet weight (1.92kg), satisfactory efficiency (~92%), while keeping the total machine weight relatively low (~82kg), as also shown in Table 2. The second alternative is given again by GA, while PSO method presents quite much magnet weight.
- c) If the PMSM copper losses, thus the efficiency, is the primary objective (CF_2), the GWO method presents the most satisfactory results, by keeping the losses the lowest possible resulting at a high-efficient motor (96.43%), whereas PSO takes the lead over GA, proposing a solution with an efficiency of 84.55% and finally GA method is the worst performing, presenting an efficiency of 82.1%.

The left part of Table 3 shows the computational costs of the adopted and applied methods. Here, the first place goes to GWO method which provides solutions in the order of magnitude of 2-3 seconds for our problem. PSO needs almost 1.5 times more computational time, while GA is the slowest optimization method with a response time of almost 10 seconds.

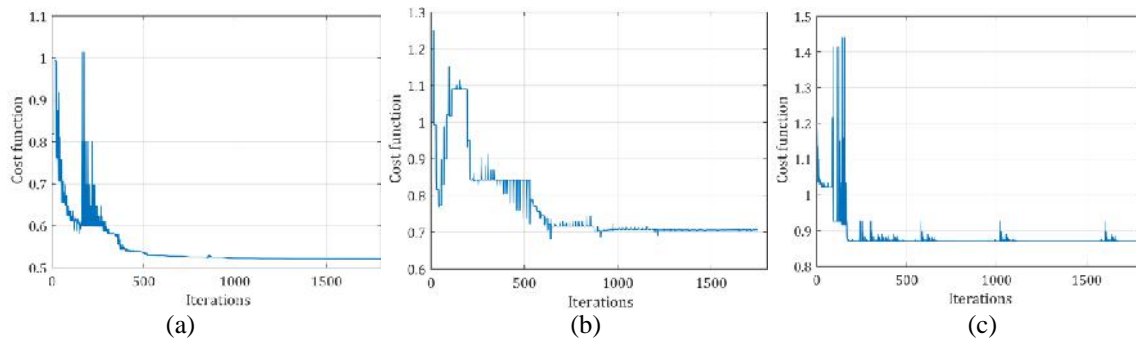


Figure 4. Convergence behavior of applied optimization methods to PMSM design problem, a) GWO, b) GA, c) PSO

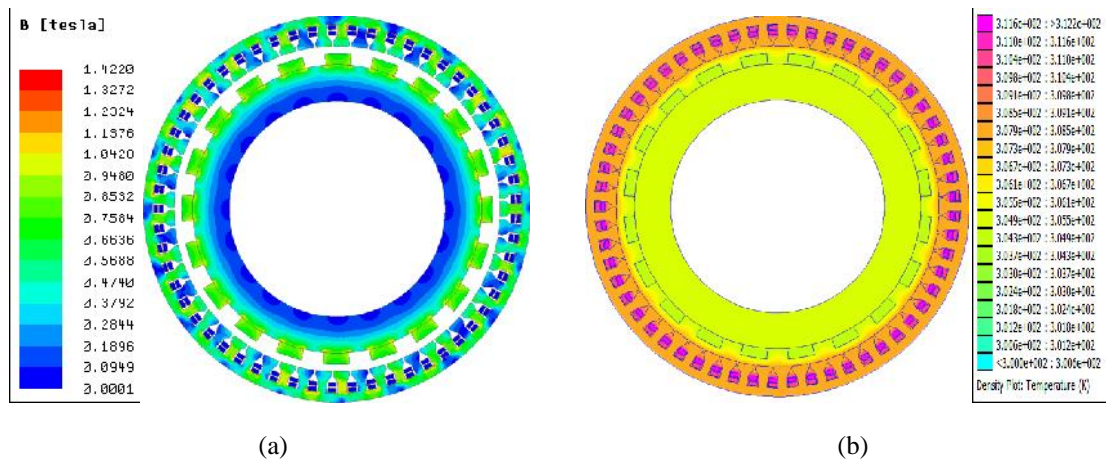


Figure 5. PMSM design obtained (CF_2) by GWO application. a) flux density distribution, b) heat density plot

Table 1. PMSM design variables results through GWO, GA and PSO optimization methods

| | G | | W | | O | | GA | | PSO | |
|-------------------|--------|--------|--------|--------|--------|--------|--------|--------|--------|--|
| | CF_1 | CF_2 | CF_3 | CF_1 | CF_2 | CF_3 | CF_1 | CF_2 | CF_3 | |
| N_m | 60 | 20 | 36 | 72 | 60 | 20 | 60 | 62 | 34 | |
| N_{spp} | 0.403 | 0.948 | 0.742 | 0.561 | 0.233 | 0.999 | 0.611 | 0.394 | 0.43 | |
| D_o (cm) | 27.88 | 27.48 | 27.65 | 24.41 | 28.74 | 37.66 | 26.58 | 28.12 | 32.52 | |
| D_r (cm) | 20.04 | 20.21 | 20.00 | 20.00 | 20.24 | 26.15 | 20.00 | 20.00 | 20.76 | |
| L (cm) | 10.02 | 17.02 | 14.71 | 10.00 | 11.79 | 10.01 | 10.40 | 12.47 | 17.46 | |
| n_s | 12 | 10 | 11 | 11 | 10 | 20 | 12 | 10 | 11 | |
| l_m (mm) | 12.77 | 10.35 | 7.88 | 7.50 | 7.40 | 10.50 | 9.87 | 10.70 | 10.25 | |
| b_{ls} (mm) | 5.31 | 6.62 | 3.01 | 2.50 | 9.70 | 8.60 | 3.52 | 3.95 | 6.10 | |
| h_{ss} (mm) | 14.19 | 15.17 | 16.95 | 9.00 | 21.40 | 22.10 | 10.95 | 17.75 | 33.40 | |
| h_{sw} (mm) | 2.01 | 7.59 | 6.67 | 2.00 | 4.80 | 5.00 | 3.10 | 2.25 | 8.65 | |
| b_{ss0}/b_{ss1} | 0.769 | 0.200 | 0.314 | 0.609 | 0.802 | 0.236 | 0.695 | 0.305 | 0.205 | |
| (mm) | 5.28 | 5.52 | 4.94 | 3.00 | 3.00 | 13.90 | 5.15 | 3.25 | 3.50 | |

Table 2. Main objective quantities results through GWO, GA and PSO optimization methods

| | GWO | | | GA | | | PSO | | |
|------------------|--------|--------|--------|--------|--------|--------|--------|--------|--------|
| | CF_1 | CF_2 | CF_3 | CF_1 | CF_2 | CF_3 | CF_1 | CF_2 | CF_3 |
| M_w^{tot} (kg) | 48.57 | 72.06 | 82.24 | 53.46 | 73.46 | 96.11 | 54.64 | 78.68 | 94.41 |
| (%) | 90.29 | 96.43 | 92.29 | 79.10 | 82.1 | 74.80 | 78.20 | 84.55 | 76.42 |
| M_m^{tot} (kg) | 2.72 | 3.68 | 1.92 | 3.54 | 3.71 | 1.93 | 4.13 | 4.48 | 2.64 |

Table 3. Computational cost of optimization methods used and corresponding PMSM design solutions' slot current density

| | Computational cost (secs) | | | Slot current density (A/cm^2) | | |
|-----|---------------------------|--------|--------|-----------------------------------|--------|--------|
| | CF_1 | CF_2 | CF_3 | CF_1 | CF_2 | CF_3 |
| GWO | 2.631 | 2.713 | 2.267 | 722 | 264 | 351 |
| GA | 10.356 | 9.295 | 9.789 | 737 | 590 | 240 |
| PSO | 3.858 | 3.951 | 3.649 | 745 | 556 | 269 |

In terms of converging, there are also interesting results. Figure 4 shows the behavior of GWO, GA and PSO convergence throughout the iterative process (CF_2 case). It can be seen that GWO converges to the 12-variable optimal combination in about 500 iterations giving a cost function value of 0.53. GA needs approximately twice iterations while trying to explore/exploit the solution search space and converges to 0.7. PSO seems to converge prematurely scoring 0.87. Our investigation continues with the thermal calculations involving slot current density for each one of the geometries. These are summarized in the right part of Table 3. It can be seen that all designs develop a current density lower than $800A/cm^2$ and can be realized as air-cooled machines (as stated in §2.2). One of the proposed by GWO algorithm optimized design (optimized for efficiency i.e. CF_2) was implemented in FEM and thermal analysis software and visualization instants of its operation under nominal load are shown in Figure 5, where the relevant geometry, the flux density distribution as well as the heat density plots are depicted. It can be seen that the maximum magnetic flux density, in any part of the machine is lower than the constraint set, with a maximum of approximately 1.42T (with a 1.6T constraint), while the maximum temperature rise is about $39^\circ C$ (without an outer enclosure/frame structure). In other words, these results from both FEM and thermal analyses are judged absolutely satisfactory.

5. CONCLUSION

The implementation of GWO into inner rotor PMSM design problem has been presented in this paper. The results obtained show that GWO have been successfully implemented to anticipate the practical constraints of PMSM design problem and provide very competitive alternative designs to replace traditional low speed induction-motor/gearbox systems, in terms of minimizing total losses and permanent magnet weight. It has been observed that the GWO has the ability to converge to a better quality optimal solutions and possesses better convergence characteristics than other prevailing techniques reported in literature. The solution provided by GWO was also evaluated through finite element analysis as well as thermal analysis procedures, where an acceptable and satisfactory performance was recorded. It is also clear from the results obtained, by several trials, that the GWO shows a good balance between exploration and exploitation, a property which result in high local optima avoidance. Thus, this algorithm may become very promising for solving complex engineering optimization problems such as the electrical machine design one.

APPENDIX

Table A1. Induction motor/gearbox data corresponding to PMSM

| Quantity | Symbol | Unit | Induction Motor | Gear-box | Total | PMSM |
|-------------------|-------------|------|-----------------|----------|-------|------|
| Outer Stator Dia. | D_o | cm | 18 | 50 | 50 | 50 |
| Machine length | L | cm | 9.5 | 40.5 | 50 | 50 |
| Machine weight | M_w^{tot} | kg | 22 | 131 | 153 | 150 |
| Efficiency | | % | 88 | 90 | 79 | 79 |
| Shaft torque | T | Nm | 28 | 1:30 | 840 | 840 |
| Shaft speed | n | rpm | 1500 | 30:1 | 50 | 50 |
| Output Power | P_{out} | kW | 4.4 | - | 4.4 | 4.4 |
| Line current | I | A | 8.6 | - | 8.6 | 8.6 |
| Supply voltage | V_{LL} | Volt | 400 | - | 400 | §2.2 |
| Frequency | f | Hz | 50 | - | 50 | §2.2 |

Table A3. Constant values involved in the PMSM design problem

| Quantity | Symbol | Set Value |
|-------------------------------|--------------|--------------------------|
| Maximum flux density (NdFeB) | B_{max} | 1.6T |
| Remanence flux density | B_r | 1.08 |
| Area occupied by conductors | k_{cp} | 0.25 |
| Operating frequency | f | 50Hz |
| Relative permeability | m_r | 1.03 |
| Motor's shaft speed | n | 50rpm |
| Mass density of the copper | P_{copper} | 8920kg/m ³ |
| No. of phases | N_{ph} | 3 |
| Mass density of the back iron | P_{bi} | 7750kg/m ³ |
| Copper resistivity | Cu | 1.72x10 ⁻⁸ /m |
| Mass density of the magnet | P_m | 7500kg/m ³ |
| Torque on the motor's shaft | T | 840Nm |
| No. of armature paths | A | 2 |

Table A2. Universe of discourse of PMSM design problem variables

| Quantity | Symbol | Variable Range |
|--|------------|-----------------|
| No. of magnet poles | N_m | 20 - 80 |
| No. of slots / pole per phase | N_{spp} | 0.001 - 1 |
| Outer Stator Diameter | D_o | 20 - 50 cm |
| Outer Rotor Diameter | D_r | 20 - D_o cm |
| Active machine length | L | 10 - 50 cm |
| No. of parallel conductor paths | n_c | 10 - 40 |
| Magnet thickness | l_m | 2 - 15 mm |
| Stator tooth width | b_{ts} | 2.5 mm |
| Stator slot height | h_{ss} | 0 mm |
| Slot wedge height | h_{sw} | 1 - h_{ss} mm |
| Stator slot b_{s0} / b_{ss1} ratio | k_{open} | 0.2 - 0.9 |
| Airgap length | | 3 - 20 mm |

Table A4. PMSM design problem inequality constraints

| Description | Symbol | Constraint |
|------------------------------|-------------|--|
| Stator yoke height | h_{sy} | $\geq h_{ss}/2$ |
| Slot wedge height | h_{sw} | $\geq 1mm$ |
| Slot opening height | h_{s0} | $\geq 2mm$ |
| Slot width | b_{ss2} | $0.15h_{ss} \leq b_{ss2} \leq 0.5h_{ss}$ |
| Tooth width | b_{ts} | $\geq 0.3 s$ |
| Slot opening width | b_{ss0} | $\geq 2mm$ |
| Flux density in stator teeth | B_{ts} | $\leq 1.6T$ |
| Flux density in stator yoke | B_{sy} | $\leq 1.4T$ |
| Flux density in rotor yoke | B_{ry} | $\leq 1.4T$ |
| Airgap flux density | B | $\leq 1.1T$ |
| Copper losses | P_{Cu} | $\leq 700W$ |
| Magnet weight | M_m^{tot} | $\leq 5.5kg$ |
| Machine weight | M_w^{tot} | $\leq 150kg$ |

REFERENCES

- [1] Waide P and Brunner C, "Energy-Efficiency Policy Opportunities for Electric Motor-Driven Systems," *International Energy Agency (IEA) Working Paper*, Paris, France, 2011. www.iea.org.
- [2] IEC 60034-30, "Rotating electrical machines - Part 30-2: Efficiency classes of variable speed AC motors," *International Electrotechnical Commission Standard*, 2013.
- [3] Lipu M. S. H. and Karim T. F., "Energy efficiency opportunities and savings potential for electric motor and its impact on GHG emissions reduction," *International Journal of Electrical and Computer Engineering*, vol/issue: 3(4), pp. 533-542, 2013.
- [4] Patel H. K., et al., "Performance comparison of permanent magnet synchronous motor and induction motor for cooling tower application," *International Journal of Emerging Technology and Advanced Engineering*, vol/issue: 2(8), pp. 167-171, 2012.
- [5] Lakshmikanth S., et al., "Noise and vibration reduction in permanent magnet synchronous motors - A review," *International Journal of Electrical and Computer Engineering*, vol/issue: 2(3), pp. 405-416, 2012.
- [6] Spooner E. and Williamson A. C., "Direct coupled, permanent magnet generators for wind turbine applications," *IEE Proceedings - Electric Power Applications*, vol/issue: 143(1), pp. 1-8, 1996.
- [7] Dubois M. R. J., "Optimized Permanent Magnet Generator Topologies for Direct-Drive Wind Turbines," *Doctoral Thesis*, TU Delft, Delft University of Technology, 2004.
- [8] Chen J. Y., et al., "Design and finite-element analysis of an outer-rotor permanent-magnet generator for directly coupled wind turbines," *IEEE Trans. on Magnetics*, vol/issue: 36(5), pp. 3802-3809, 2000.
- [9] Krøvel Ø., et al., "Design of an integrated 100kW permanent magnet synchronous machine in a prototype thruster for ship propulsion," in *Proc. of the 16th Int. Conference on Electrical Machines (ICEM)*. Cracow, Poland, Sep. 5-8, 2004, cd.ref. 697.
- [10] Ficheux R., et al., "Axial-flux permanent-magnet motor for direct-drive elevator systems without machine room," *IEEE Transactions on Industry Applications*, vol/issue: 37(6), pp. 1693-1701, 2001.
- [11] Peroutka Z., et al., "Control of permanent magnet synchronous machine wheel drive for low-floor tram," in *Proc. of 13th European Conference on Power Electronics and Applications (EPE)*, Barcelona, Spain, 8-10 Sep, vol. 1, pp. 1-9, 2009.
- [12] Meier F., "Permanent-magnet synchronous machines with non-overlapping concentrated windings for low-speed direct-drive applications," *Doctoral Thesis*, Royal Institute of Technology, KTH, Stockholm, 2008.
- [13] Libert F. and Soulard J., "Design study of a direct-driven surface mounted permanent magnet motor for low speed application," in *Proc. of the 5th International Symposium on Advanced Electromechanical Motion Systems - (Electromotion)*, Marrakesh, Morocco, 26-28 Nov, vol. 1, 2003.

- [14] El-Sawy A. A., *et al.*, "A novel hybrid ant colony optimization and firefly algorithm for solving constrained engineering design problems," *Journal of Natural Sciences and Mathematics*, vol/issue: 6(1), pp. 1-22, 2013.
- [15] Tušar T., *et al.*, "A comparative study of stochastic optimization methods in electric motor design," *Applied Intelligence*, vol. 27, pp. 101-111, 2007.
- [16] Mouellef S., *et al.*, "Optimal design of switched reluctance motor using PSO based FEM-EMC modeling," *International Journal of Electrical and Computer Engineering*, vol/issue: 5(5), pp. 887-895, 2015.
- [17] Ab-Wahab M. N., *et al.*, "A comprehensive review of swarm optimization algorithms," *Public Library of Science One (PLoS One)*, vol/issue: 10(5), pp. 1-36, 2015.
- [18] Lin L. and Gen M., "Auto-tuning strategy for evolutionary algorithms: balancing between exploration and exploitation," *Soft Computing*, vol. 13, pp. 157-168, 2009.
- [19] Mirjalili S., *et al.*, "Grey Wolf Optimizer," *Advances in Engineering Software*, vol. 69, pp. 46-61, 2014.
- [20] El-Nasser G., *et al.*, "A comparative study of meta-heuristic algorithms for solving quadratic assignment problem," *Intern. Journal of Advanced Computer Science and Applications*, vol/issue: 5(1), pp. 1-6, 2014.
- [21] Karnavas Y. L. and Korkas C. D., "Optimization methods evaluation for the design of radial flux surface PMSM," in *Proc. of the XXIth Intl. Conference on Electrical Machines (ICEM), Berlin, Germany, 2-5 Sept*, vol. 1, pp. 1348-1355, 2014.
- [22] Pyrhonen J., *et al.*, "Design of Rotating Electrical Machines," 2nd ed., John Wiley & Sons, 2013.
- [23] Magnussen F. and Sadarangani C., "Winding factors and Joule losses of permanent magnet machines with concentrated windings," in *Proc. of IEEE International Electric Machines & Drives Conference (IEMDC), Madison, Wisconsin*, vol. 1, pp. 333-339, 2003.
- [24] Sun W. and Yuan Y. X., "Optimization Theory and Methods: Nonlinear Programming," *Springer Optimization and Its Applications Book Series, Springer*, vol. 1, pp. 541, 2010.
- [25] Mitsuo G. and Runwei C., "Genetic Algorithms and Engineering Optimization," John Wiley & Sons, Canada, 2000.
- [26] Poli R., "Analysis of the publications on the applications of particle swarm optimisation," *Journal of Artificial Evolution and Applications*, pp. 1-10, 2008.

BIOGRAPHIES OF AUTHORS



Yannis L. Karnavas was born in Volos, Hellas, 1969. He received the Diploma Degree and his Ph.D. from the Dept. of Electrical & Computer Engineering (DECE), Democritus University of Thrace (DUTH), Xanthi, Hellas in 2002. He is with the Electrical Machines Laboratory of the DECE, DUTH as an Assistant Professor. His research interests include electrical machines design, analysis, modeling and optimization, controller design and application to electrical machines and artificial intelligence methods application to them. He has published several papers in various international journals and conferences as well as book chapters in international engineering books. He has participated in many research projects as research leader or scientific associate. He serves as an Associate Editor and as an Editorial board member in various international scientific journals. He is a chartered electrical engineer as well as a member of Hellenic Technical Chamber. Prof. Karnavas is also an IEEE PES, IAS and IES member.



Ioannis D. Chasiotis was born in Athens, Hellas, 1991. He received the Diploma Degree in electrical and computer engineering from the Department of Electrical and Computer Engineering, Democritus University of Thrace, Xanthi, Hellas. He is with the Electrical Machines Laboratory of the same Dept. where he is currently pursuing his Ph.D. degree. His research interests are in the area of electrical machines design and the development of relevant optimization methods and applications. He is a recipient of 3-year award scholarship from Bodossaki Foundation for his post-graduate studies. He is student member of IEEE.



Emmanouil L. Peponakis was born in Heraklion, Hellas, 1992. He is with the Electrical Machines Laboratory of the Department of Electrical and Computer Engineering, Democritus University of Thrace, Xanthi, Hellas, whereas he is currently pursuing the Diploma Degree in electrical and computer engineering. His research interests are in the areas of electrical machines design, thermal analysis of electrical machines and hard magnetic materials behavior on permanent magnet machines, as well as their applications.